OPTIMAL GEOMETRY ANALYSIS FOR ELLIPTIC TARGET LOCALIZATION BY MULTISTATIC RADAR WITH INDEPENDENT BISTATIC CHANNELS

Ngoc Hung Nguyen[⋆] *and Kutluyıl Doğançay*[†⋆]

[⋆]Institute for Telecommunications Research, [†]School of Engineering
University of South Australia, Mawson Lakes SA 5095, Australia

ABSTRACT

This paper derives the optimal angular geometry for elliptic time-of-arrival localization by a multistatic radar consisting of multiple independent bistatic channels. The optimal geometry analysis is conducted based on minimization of the area of the estimation confidence region which is equivalent to maximizing the determinant of the Fisher information matrix. It is shown that the optimal angular geometry is obtained when the transmitter and receiver of each bistatic channel are collinear with the target where the target is placed at the either end. The optimization problem therefore boils down to determination of the optimal angular separation between different bistatic channels which is mathematically equivalent to the optimal angular sensor separation for angle-of-arrival localization. These analytical results are confirmed by simulation examples.

Index Terms— Optimal sensor placement, elliptic TOA localization, bistatic radar, multistatic radar, Fisher information matrix

1. INTRODUCTION

The classical problem of target localization continues to receive great attention due to its importance to a wide range of applications in wireless communication systems, sonar and radar, and surveillance and navigation systems [1–13]. The most common localization techniques are developed based on time of arrival (TOA) [1–6], time difference of arrival (TDOA) [5–8], angle of arrival (AOA) [4, 8, 9], Doppler shift [10, 11], and received signal strength (RSS) [12]. The TOA-based localization can be further categorized into the circular-TOA-based method [3, 5, 6] and the elliptic-TOA-based method [1–3]. The circular-TOA-based localization utilizes the propagation times of the transmitted signals travelling from a radiating source to passive sensors to estimate the source location [5, 6]. This method can also be employed for the target localization by netted monostatic radars [3]. On the other hand, the elliptic-TOA-based localization relies on the propagation times of the transmitted signals travelling from transmitters to the target and reflected back to receivers, where the transmitters and receivers are located separately at different positions [2]. The target location estimate can be therefore obtained by the intersection of the ellipses (in 2D) or the ellipsoids (in 3D) with the foci at the transmitter and receiver positions. The elliptic localization is commonly used in multistatic radar [3], multistatic sonar [13], and MIMO radar systems [14].

The relative sensor-target geometry is known to be an important factor that significantly affects the performance of target localization [15]. Extensive research has been conducted to identify the optimal sensor placement for different target localization problems (e.g., the AOA-based localization in [9,15,16], the circular-TOA-based localization in [15, 16], the TDOA-based localization in [17, 18], and the RSS-based localization in [12, 16]), where the maximization of the determinant of the Fisher information matrix is commonly utilized as the optimality criterion.

In contrast to other localization techniques, the optimal sensor placement for the elliptic-TOA-based localization has not been fully examined. A geometric dilution of precision (GDOP)-based analysis was reported in [19] by modelling each bistatic channel of a multistatic radar system as a virtual monostatic radar. The optimum receiver placement for a specific case of one transmitter and multiple receivers appeared in [2] with equal noise variances at different receivers and even number of receivers. The optimum placement of multiple transmitters and multiple receivers under MIMO radar configuration was considered in [14], where the noise levels at different receivers are assumed to be the same and the numbers of transmitters and receivers are both larger than three. In both [2, 14], the optimality was obtained by minimizing the trace of the Cramér-Rao lower bound (CRLB) matrix. Another related work on the optimal geometry design for multistatic sensors appeared in [20], in which an algorithm was proposed to find the local optimal geometry. Moreover, [20] is computationally expensive and generally does not guarantee a global optimal solution.

This paper aims to theoretically analyse the optimal angular geometry for the elliptic-TOA-based localization in the 2D plane by a multistatic radar consisting of multiple independent bistatic channels. In this configuration, two or more transmitters of different type (e.g., monopulse, continuous-wave) operating in different frequency bands (e.g., L-, S-, C-, X-bands, etc.) are individually coupled with different receivers, hence forming independent bistatic channels. The presented analysis allows the measurement noise variances to be either equal or unequal at different receivers. The optimality criterion chosen for the analysis is to minimize the area of estimation confidence region by maximizing the determinant of the Fisher information matrix (FIM), which is known as the D-optimality criterion [21]. Other criteria are also available such as the A-optimality criterion, which minimizes the trace of the CRLB (the inverse of FIM), and the E-optimality criterion, which minimizes the maximum eigenvalue of the CRLB matrix. However, these two criteria are affected by scale changes in the parameters as well as linear transformations of the output [21]. In contrast, the D-optimality criterion is invariant under these transformations [21], hence the D-optimality criterion is adopted as the criterion for the optimal geometry analysis in this paper. Note that the presented work differs from [2, 14] in terms of system configurations as well as optimality criteria, therefore leading to a different characterization of optimal angular geometries. It is shown that the optimal angular geometry for the considered multistatic radar setting is obtained when the transmitter and receiver of each of the bistatic channels are collinear with the target where the target is placed at either end. The optimization problem then becomes determining the optimal angular separation between different bistatic channels. For $N = 2$, the

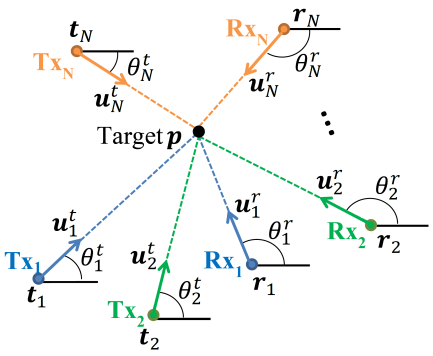

Fig. 1. The considered 2D elliptic-TOA-based target localization.

optimal geometry is obtained when the line of sight (LOS) lines of the two channels are perpendicular. For $N = 3$, the solutions for the optimal geometry are shown in Section 3. For $N \geq 4$, infinitely many optimal configurations exist if $2/\sigma_{\min}^2 > \sum_1^N 1/\sigma_i^2$ does not hold where $\sigma_{\min} = \min\{\sigma_1, \ldots, \sigma_N\}$ and σ_i^2 is the measurement error covariance at the i-th bistatic channel. These optimal configurations can be identified by grouping the bistatic channels into smaller clusters with two or three channels and optimizing the angular separation within each cluster. It should be noted that the rotation of the optimized clusters does not affect the optimality of the overall system. To confirm the validity of the theoretical analysis, simulation examples for UAV path optimization are presented in Section 4.

2. PROBLEM STATEMENT

We consider a 2D elliptic-TOA-based target localization by a multistatic radar which consists of N independent bistatic channels Tx_i–Rx_i with $i = 1, 2, ..., N$. The localization problem is depicted in Fig. 1, where $\mathbf{p} = [p_x, p_y]^T$ is the unknown target location with ^{T} denoting matrix transpose, $\mathbf{t}_i = [x_i^t, y_i^t]^T$ and $\mathbf{r}_i = [x_i^r, y_i^r]^T$ are the transmitter and receiver positions, respectively, of the i-th bistatic channel. The TOA measurement τ_i of the i-th bistatic channel is given by

$$\tilde{\tau}_i(\mathbf{p}) = \tau_i(\mathbf{p}) + e_i, \text{ with } \tau_i(\mathbf{p}) = \frac{\|\mathbf{p} - \mathbf{t}_i\| + \|\mathbf{p} - \mathbf{r}_i\|}{c} \quad (1)$$

where c is the speed of propagation for the transmitted signal, $\|\cdot\|$ denotes the Euclidean norm, and e_i is the TOA measurement error which is modelled as a zero-mean independent Gaussian noise. The error covariance $E\{e_i^2\}$ is usually a function of the target-transmitter and target-receiver distances among other things. The TOA measurement can be obtained by performing the cross-correlation between the reflected-from-target signal and the transmitted signal in active bistatic radars [22] or the cross-correlation between the reflected-from-target signal and the LOS signal from the transmitter in passive bistatic radars [23].

The total range measurement $\tilde{d}_i$ from the target to the transmitter and receiver of the i-th channel can therefore be expressed as

$$\tilde{d}_i(\mathbf{p}) = d_i(\mathbf{p}) + n_i, \text{ with } d_i(\mathbf{p}) = \|\mathbf{p} - \mathbf{t}_i\| + \|\mathbf{p} - \mathbf{r}_i\| \quad (2)$$

where $n_i = ce_i$ is the range measurement error with $E\{n_i^2\} = \sigma_i^2$ (i.e., $E\{e_i^2\} = \sigma_i^2/c^2$). Writing the range measurement equation in vector form gives

$$\tilde{\mathbf{d}} = \mathbf{d}(\mathbf{p}) + \mathbf{n} = [d_1, d_2, \ldots, d_N]^T + [n_1, n_2, \ldots, n_N]^T \quad (3)$$

with the covariance matrix of the range measurements given by

$$\mathbf{\Sigma} = E\{\mathbf{n}\mathbf{n}^T\} = \mathrm{diag}(\sigma_1^2, \sigma_2^2, \ldots, \sigma_N^2). \quad (4)$$

Solving (3) requires at least two equations (i.e., $N \geq 2$) as there are two unknowns p_x and p_y. However, two equations do not provide a unique solution for the target position because two ellipses may intersect at two distinct points. Therefore, at least three equations are required to ensure the uniqueness of the solution (i.e., $N \geq 3$) [2].

With the independent Gaussian noise for the TOA measurement error, the FIM for the target localization is

$$\mathbf{\Phi} = \begin{bmatrix} \phi_{11} & \phi_{12} \\ \phi_{21} & \phi_{22} \end{bmatrix} = \mathbf{J}_0^T \mathbf{\Sigma}^{-1} \mathbf{J}_0 \quad (5)$$

where $\mathbf{J}_0$ is the Jacobian matrix of (3) evaluated at the true target location

$$\mathbf{J}_0 = \begin{bmatrix} (\mathbf{u}_1^t + \mathbf{u}_1^r)^T \\ (\mathbf{u}_2^t + \mathbf{u}_2^r)^T \\ \vdots \\ (\mathbf{u}_N^t + \mathbf{u}_N^r)^T \end{bmatrix}, \ \mathbf{u}_i^t = \begin{bmatrix} \cos\theta_i^t \\ \sin\theta_i^t \end{bmatrix}, \ \mathbf{u}_i^r = \begin{bmatrix} \cos\theta_i^r \\ \sin\theta_i^r \end{bmatrix}. \quad (6)$$

In (6), $\mathbf{u}_i^t$ and $\mathbf{u}_i^r$ are the unit vectors pointing to the target as shown in Fig. 1. From (4)–(6), the FIM becomes

$$\mathbf{\Phi} = \sum_{i=1}^{N} \frac{1}{\sigma_i^2} (\mathbf{u}_i^t + \mathbf{u}_i^r)(\mathbf{u}_i^t + \mathbf{u}_i^r)^T. \quad (7)$$

As discussed in Section 1, we adopt the maximization of determinant of FIM as the criterion to derive the optimal angular geometry for the considered elliptic target localization. Since the area of the 1-σ error ellipse (i.e., 39.4% uncertainty region) of an efficient estimator is $A_{1\sigma} = \pi/|\mathbf{\Phi}|^{1/2}$ (note that $|\cdot|$ denotes matrix determinant), maximizing the determinant of FIM is equivalent to minimizing the area of uncertainty ellipse [9]. In this paper, we assume that the elliptic localization algorithm under consideration is nearly efficient and unbiased so that its CRLB (i.e., the inverse of FIM) can be used to approximate the error covariance of the target position estimate.

Observation 1. *Reflecting both the transmitter and receiver of a bistatic channel about the target (i.e., moving Tx_i from $\mathbf{t}_i$ to $2\mathbf{p} - \mathbf{t}_i$ and Rx_i from $\mathbf{r}_i$ to $2\mathbf{p} - \mathbf{r}_i$) does not affect FIM.*

It is easy to verify this observation by substituting $\mathbf{t}_i$ by $2\mathbf{p} - \mathbf{t}_i$ and $\mathbf{r}_i$ by $2\mathbf{p} - \mathbf{r}_i$ in (7). This substitution results in $(\mathbf{u}_i^t + \mathbf{u}_i^r)$ becoming $-(\mathbf{u}_i^t + \mathbf{u}_i^r)$ which does not change FIM. This observation is useful to generate new optimal geometries from a given optimal geometry configuration by reflecting some bistatic channels about the target location.

3. OPTIMAL GEOMETRY ANALYSIS

The entries of FIM, after some algebraic manipulations, can be expressed as

$$\phi_{11} = 2\sum_{i=1}^{N} \frac{1}{\sigma_i^2} \left[1 + \cos(\theta_i^t + \theta_i^r)\right] \cos^2\left(\frac{\theta_i^t - \theta_i^r}{2}\right) \quad (8a)$$

$$\phi_{22} = 2\sum_{i=1}^{N} \frac{1}{\sigma_i^2} \left[1 - \cos(\theta_i^t + \theta_i^r)\right] \cos^2\left(\frac{\theta_i^t - \theta_i^r}{2}\right) \quad (8b)$$

$$\phi_{12} = \phi_{21} = 2\sum_{i=1}^{N} \frac{1}{\sigma_i^2} \sin(\theta_i^t + \theta_i^r) \cos^2\left(\frac{\theta_i^t - \theta_i^r}{2}\right). \quad (8c)$$

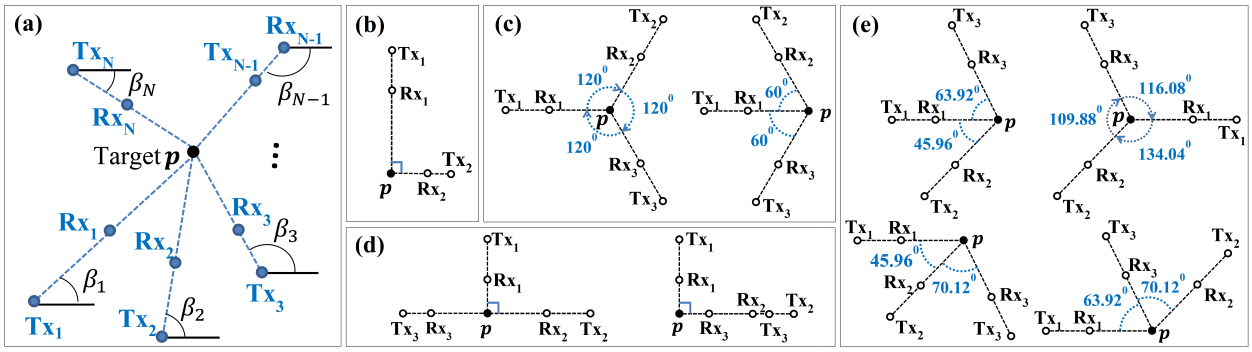

Fig. 2. (a) Angular separation between different bistatic channels; (b)–(e) Illustrations of optimal angular geometries for (b) $N = 2$, (c) $N = 3$ with equal error variances, (d) $N = 3$ with unequal error variances such that the condition (14) holds, and (e) $N = 3$ with unequal error variances $\sigma_1 : \sigma_2 : \sigma_3 = 10 : 9 : 8$.

The determinant of FIM is therefore given by

$$|\mathbf{\Phi}| = 4\left\{\left[\sum_{i=1}^{N}\frac{1}{\sigma_i^2}\cos^2\left(\frac{\theta_i^t-\theta_i^r}{2}\right)\right]^2 - \left[\sum_{i=1}^{N}\frac{1}{\sigma_i^2}\cos^2\left(\frac{\theta_i^t-\theta_i^r}{2}\right)\cos(\theta_i^t+\theta_i^r)\right]^2 - \left[\sum_{i=1}^{N}\frac{1}{\sigma_i^2}\cos^2\left(\frac{\theta_i^t-\theta_i^r}{2}\right)\sin(\theta_i^t+\theta_i^r)\right]^2\right\}. \quad (9)$$

Using the equality of $(\sum_1^N a_i)^2 = \sum_1^N a_i^2 + 2\sum_{\{i,j\}\in\mathcal{C}} a_i a_j$ and the parameter transformation of $\alpha_i = (\theta_i^t - \theta_i^r)/2$ and $\beta_i = (\theta_i^t + \theta_i^r)/2$, the determinant of FIM becomes

$$|\mathbf{\Phi}| = 16\sum_{\{i,j\}\in\mathcal{C}}\frac{1}{\sigma_i^2\sigma_j^2}\cos^2(\alpha_i)\cos^2(\alpha_j)\sin^2(\beta_i-\beta_j) \quad (10)$$

where $\mathcal{C}$ is all 2-combinations of the set $S = \{1, 2, \ldots, N\}$ (note that there are $C_N^2 = \frac{N!}{2!(N-2)!}$ combinations of $\{i, j\}$).

It is apparent that α_i and β_i become independent variables after the above parameter transformation. Therefore, for any particular values of β_i with $i = 1, 2, \ldots, N$, we always have

$$|\mathbf{\Phi}| \le 16\sum_{\{i,j\}\in\mathcal{C}}\frac{1}{\sigma_i^2\sigma_j^2}\sin^2(\beta_i-\beta_j) \quad (11)$$

with the equality holding when $\cos^2(\alpha_i) = 1$ for all $i = 1, 2, \ldots, N$ (i.e., $\alpha_i = 0$ or $\alpha_i = \pi$; hence $\theta_i^t = \theta_i^r = \beta_i$). As a result, the optimal angular geometry is obtained when the transmitter and receiver of each bistatic channel are collinear with the target where the target is placed at either end, i.e., $\theta_i^t = \theta_i^r = \beta_i$ for all $i = 1, 2, \ldots, N$. The optimization problem now reduces to finding the optimal angular separation between different bistatic channels as shown in Fig. 2(a).

As a parenthetical remark, for the case when the transmitter, receiver and target are collinear for any $(N-1)$ bistatic channels with the target in between the transmitter and receiver (i.e., $\cos^2(\alpha_i) = \cos^2(\pm\pi/2) = 0$ for all $i \in \mathcal{C}_{N-1}$ where $\mathcal{C}_{N-1}$ is any combination of $(N-1)$ channels), we have $|\mathbf{\Phi}| = 0$ which represents a bad geometry.

We formally have the following results:

Theorem 1. *Maximizing the determinant of FIM is equivalent to*

$$\max_{\boldsymbol{\beta}}\left\{\left[\sum_{i=1}^{N}\frac{1}{\sigma_i^2}\right]^2 - \left[\sum_{i=1}^{N}\frac{\sin(2\beta_i)}{\sigma_i^2}\right]^2 - \left[\sum_{i=1}^{N}\frac{\cos(2\beta_i)}{\sigma_i^2}\right]^2\right\} \quad (12)$$

where $\boldsymbol{\beta} = [\beta_1, \beta_2, \ldots, \beta_N]$ *and* $\theta_i^t = \theta_i^r = \beta_i$.

Note that (12) is obtained by substituting $\theta_i^t = \theta_i^r = \beta_i$ into (9). This optimization problem is mathematically equivalent to the optimal angular sensor separation problem for AOA localization in [9] and its solutions are summarized below:

- For $N = 2$, $|\beta_1 - \beta_2| = \pi/2$ is the optimal angular geometry, i.e., the LOS lines of the two channels are perpendicular, as illustrated in Fig. 2(b).
- For $N = 3$, the optimal solutions are

$$\beta_2 - \beta_1 = \pm\tan^{-1}(\sqrt{\zeta}, b^2 - a^2 - 1)/2 \quad (13a)$$

$$\beta_3 - \beta_1 = \mp\tan^{-1}(\sqrt{\zeta}, a^2 - b^2 - 1)/2 \quad (13b)$$

  where $a = (\sigma_1/\sigma_2)^2$, $b = (\sigma_1/\sigma_3)^2$, and $\zeta = -(a+b+1)(a-b+1)(a+b-1)(a-b-1)$, and $\tan^{-1}(y, x)$ is the four-quadrant inverse tangent of y/x. By reflecting each of the bistatic channels about the target location, four distinct optimal angular geometries can be obtained (see Fig. 2(e) for an example). However, if $m \in \{1, 2, 3\}$ exists such that

$$1/\sigma_m^2 > \sum_{1\le i\le 3, i\ne m} 1/\sigma_i^2, \quad (14)$$

  we have $\zeta < 0$, hence (13) yields complex solutions and cannot be used. In this case, the optimal solutions are instead given by $\beta_k = \pm\pi/2 + \beta_m$ with $k \in \{1, 2, 3\}\backslash m$ as illustrated in Fig. 2(d), where $\backslash$ denotes set subtraction.
- For $N \ge 4$, there are infinitely many solutions for the optimization problem (12) when $2/\sigma_m^2 > \sum_1^N 1/\sigma_i^2$ does not hold with $m = \arg\min_{(i)} \sigma_i$ (if this condition holds, the solutions are $\beta_k = \pm\pi/2 + \beta_m$ with $k \in \{1, \ldots, N\}\backslash m$) [9]. The solutions can be identified as in Section 4 of [9]. Alternatively, the optimal angular configuration can be identified by grouping the bistatic channels into smaller clusters with two or three channels and optimizing the angular separation within each cluster [9]. The optimality is not affected by the rotation of the optimized clusters, hence an infinite number of optimal configurations exists [9].

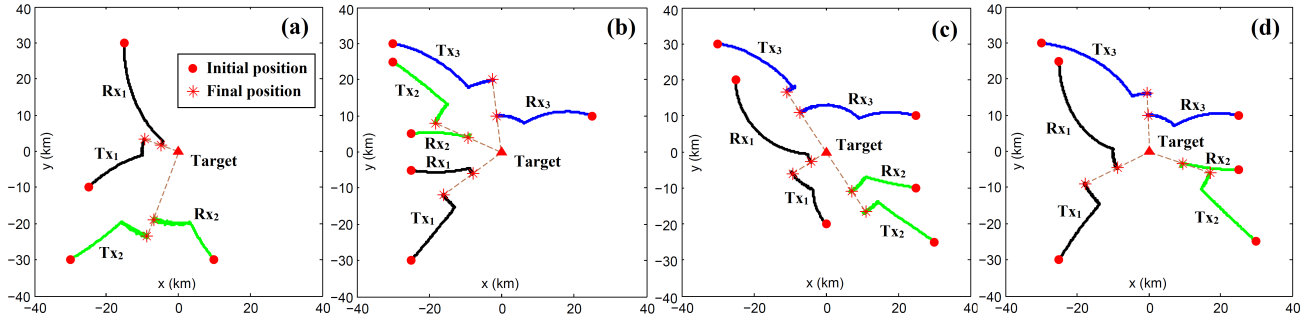

Fig. 3. The optimal trajectories of transmitters and receivers using the gradient-descent trajectory optimization for: (a) two bistatic channels ($N = 2$) with $d_1^T = 10$ km, $d_2^T = 25$ km, $d_1^R = 5$ km, and $d_2^R = 20$ km, (b) three bistatic channels ($N = 3$) with $d_1^T = d_2^T = d_3^T = 20$ km and $d_1^R = d_2^R = d_3^R = 10$ km, (c) $N = 3$ with $d_1^T = 11$ km, $d_2^T = d_3^T = 20$ km, $d_1^R = 5$ km, and $d_2^R = d_3^R = 13$ km, (d) $N = 3$ with $d_1^T = 20$ km, $d_2^T = 18$ km, $d_3^T = 16$ km, and $d_1^R = d_2^R = d_3^R = 10$ km.

For the case of equal error variances ($\sigma_1 = \sigma_2 = \cdots = \sigma_N$), the equal angular separation between different bistatic channels ($N \geq 3$) is one solution among other solutions which can be obtained as described above (see Fig. 2(c) for an example).

It should be noted that the collinearity between the transmitter, receiver and target for each bistatic channel does not block the radar signal travelling from the transmitter to target and reflected to the receiver because the 2D scenario is an approximation for the actual 3D scenario in practice. The 2D approximation is commonly used in the literature for low elevation-angle targets. If the transmitter and receiver of a bistatic channel have the same distance to the target, the bistatic channel is equivalent to a TOA monostatic radar.

4. SIMULATION EXAMPLES

In this section, the analytical results of the optimal angular geometry for a multistatic radar system with independent bistatic channels are confirmed by simulation examples on UAV (unmanned aerial vehicle) path optimization. UAVs are used in the simulations as the moving transmitter and receiver platforms of the multistatic radar system to localize a stationary target at $\mathbf{p} = [0, 0]^T$ km. The iterative linearized least squares estimator [8] is employed to estimate the target position using the elliptic TOA measurements. The trajectories of the transmitter and receiver platforms are optimized in order to maximize the determinant of FIM using the gradient-descent trajectory optimization [24], where the target position estimate in the previous iteration is employed to update the transmitter and receiver positions. The error variance for the TOA measurement at the i-th bistatic channel is range-dependent and modelled as $E\{e_i^2\} = \varrho_0^2(R_{Ti}^2 R_{Ri}^2)/R_0^4$ [3], where R_{Ti} and R_{Ri} are the transmitter-target and receiver-target distances respectively, $R_0 = 20$ km is the reference range, and the constant ϱ_0 is 1 μs. The first-order finite difference approximation is used to compute the gradient of FIM with the constant in (28) of [24] is $\Delta = 100$ m. The maximum UAV speed is 30 m/s, and the time step is $\Delta_t = 10$ s (i.e., the UAVs can move a maximum distance of 300 m in one time step). Each of the UAVs is subjected to a hard constraint which forces the UAV to maintain a certain clearance from the target. Let d_i^T and d_i^R denote the minimum allowed distances from the transmitter and the receiver to the target, respectively, for the i-th bistatic channel.

Fig. 3 shows the optimal trajectories of the transmitter and receiver platforms (UAVs) for four different scenarios. It is observed that, in addition to moving to locations that form optimal angular separation, the UAVs tend to move toward the target location because the measurement error variance reduces when the transmitters and receivers get closer to the target. After reaching the minimum allowed distances from the target, the UAVs move around the hard constraints until they form an optimal angular separation. Note that the optimal configuration, that is obtained by the UAVs, depends on the initial positions of the UAVs.

As can be seen in Fig. 3, the final transmitter and receiver positions of each bistatic channel are collinear with the target position where the target is placed at the either end. This observation agrees with the analytical result in Section 3. For the case of two bistatic channels, the final angular separation is approximately 90^o as shown in Fig. 3(a) which matches the analytical result in Fig. 2(b). The final angular separation between three bistatic channels in Fig. 3(b) matches the optimal angular configuration on the right-hand side of Fig. 2(c). This can be explained by noting that, in this scenario, the receivers have the same hard constraint of 10 km, and the transmitters have the same hard constraint of 20 km, hence the error variances are equal when all transmitters and receivers reach their hard constraints. In addition, the final angular separation in Fig. 3(c) matches the optimal angular geometry on the left-hand side of Fig. 2(d), where the hard constraints in this scenario satisfy the condition (14). Finally, the angular separation of 133.20^0, 110.43^0 and 116.37^0 in Fig 3(d) approximately matches the angular separation of 134.04^0, 109.88^0 and 116.08^0 of the configuration on the upper right-hand side of Fig. 2(e). Here the error variance ratios are $\sigma_1 : \sigma_2 : \sigma_3 = 10 : 9 : 8$ when all the UAVs reach their hard constraints (i.e., the same as the example in Fig. 2(e)). The small differences between the simulation and analytical results are due to the fact that, in the simulations, the determinant of FIM is computed from the estimate of the target position obtained from the previous iteration because the true target position is unknown.

5. CONCLUSION

In this paper, optimal angular geometries for elliptic-TOA-based target localization by a multistatic radar system with multiple independent bistatic channels have been derived using the criterion of minimizing the the area of the estimation confidence region. Our analysis shows that the optimal angular geometry is obtained when the transmitter and receiver of each bistatic channel are collinear with the target where the target is placed at the either end. The optimization problem then becomes the optimal angular separation problem between different bistatic channels. Simulation examples are also presented in the paper to verify the analytical results.

6. REFERENCES

[1] J. Shen, A.F. Molisch, and J. Salmi, "Accurate passive location estimation using TOA measurements," *IEEE Trans. Wireless Commun.*, vol. 11, no. 6, pp. 2182–2192, June 2012.

[2] L. Rui and K.C. Ho, "Elliptic localization: Performance study and optimum receiver placement," *IEEE Trans. Signal Process.*, vol. 62, no. 18, pp. 4673–4688, Sept 2014.

[3] A. Farina and E. Hanle, "Position accuracy in netted monostatic and bistatic radar," *IEEE Trans. Aerosp. Electron. Syst.*, vol. 19, no. 4, pp. 513–520, July 1983.

[4] N.H. Nguyen, K. Dogancay, and L.M. Davis, "Adaptive waveform and Cartesian estimate selection for multistatic target tracking," *Signal Process.*, vol. 111, no. 0, pp. 13–25, 2015.

[5] A. Beck, P. Stoica, and J. Li, "Exact and approximate solutions of source localization problems," *IEEE Trans. Signal Process.*, vol. 56, no. 5, pp. 1770–1778, May 2008.

[6] S. Chen and K.C. Ho, "Achieving asymptotic efficient performance for squared range and squared range difference localizations," *IEEE Trans. Signal Process.*, vol. 61, no. 11, pp. 2836–2849, June 2013.

[7] K. Dogancay and A. Hashemi-Sakhtsari, "Target tracking by time difference of arrival using recursive smoothing," *Signal Process.*, vol. 85, no. 4, pp. 667–679, 2005.

[8] D.J. Torrieri, "Statistical theory of passive location systems," *IEEE Trans. Aerosp. Electron. Syst.*, vol. 20, no. 2, pp. 183–198, March 1984.

[9] K. Dogancay and H. Hmam, "Optimal angular sensor separation for AOA localization," *Signal Process.*, vol. 88, no. 5, pp. 1248–1260, 2008.

[10] Y.T. Chan and F.L. Jardine, "Target localization and tracking from Doppler-shift measurements," *IEEE J. Ocean. Eng.*, vol. 15, no. 3, pp. 251–257, Jul 1990.

[11] I. Shames, A.N. Bishop, M. Smith, and B.D.O. Anderson, "Doppler shift target localization," *IEEE Trans. Aerosp. Electron. Syst.*, vol. 49, no. 1, pp. 266–276, Jan 2013.

[12] A.N. Bishop and P. Jensfelt, "Optimality analysis of sensor-target geometries for signal strength based localization," in *Proc. ISSNIP'07*, 2009, pp. 127–132.

[13] S. Coraluppi, "Multistatic sonar localization," *IEEE J. Ocean. Eng.*, vol. 31, no. 4, pp. 964–974, Oct 2006.

[14] H. Godrich, A.M. Haimovich, and R.S. Blum, "Target localization accuracy gain in MIMO radar-based systems," *IEEE Trans. Inf. Theory*, vol. 56, no. 6, pp. 2783–2803, June 2010.

[15] A.N. Bishop, B. Fidan, B.D.O. Anderson, K. Dogancay, and P.N. Pathirana, "Optimality analysis of sensor-target localization geometries," *Automatica*, vol. 46, no. 3, pp. 479–492, 2010.

[16] S. Zhao, B.M. Chen, and T.H. Lee, "Optimal sensor placement for target localisation and tracking in 2D and 3D," *Int. J. of Control*, vol. 86, no. 10, pp. 1687–1704, 2013.

[17] K. Dogancay and H. Hmam, "On optimal sensor placement for time-difference-of-arrival localization utilizing uncertainty minimization," in *Proc. EUSIPCO*, 2009, pp. 1136–1140.

[18] K.W.K. Lui and H.C. So, "A study of two-dimensional sensor placement using time-difference-of-arrival measurements," *Digital Signal Process.*, vol. 19, no. 4, pp. 650 – 659, 2009.

[19] N.J. Willis, H.D. Griffiths, and D.K. Barton, "Air surveillance," in *Advances in Bistatic Radar*, N.J. Willis and H.D. Griffiths, Eds., chapter 6. SciTech Publishing, Raleigh, NC, 2007.

[20] R. Fogle and B.D. Rigling, "Optimal geometry designs for unconstrained and topologically-constrained multistatic sensors," in *Proc. 40th Asilomar Conf. Signals, Syst., Comput.*, Oct 2006, pp. 1570–1574.

[21] D. Ucinski, *Optimal Measurement Methods for Distributed Parameter System Identification*, CRC Press, Boca Raton, 2004.

[22] M.I. Skolnik, *Radar Handbook*, McGraw-Hill, New York, 1990.

[23] H.D. Griffiths and C.J. Baker, "Passive coherent location radar systems. part 1: performance prediction," *IEE Proc., Radar Sonar Navig.*, vol. 152, no. 3, pp. 153–159, 2005.

[24] K. Dogancay, "Online optimization of receiver trajectories for scan-based emitter localization," *IEEE Trans. Aerosp. Electron. Syst.*, vol. 43, no. 3, pp. 1117–1125, July 2007.